First Quantification of Electron Thermal Transport in the MST Reversed-Field Pinch

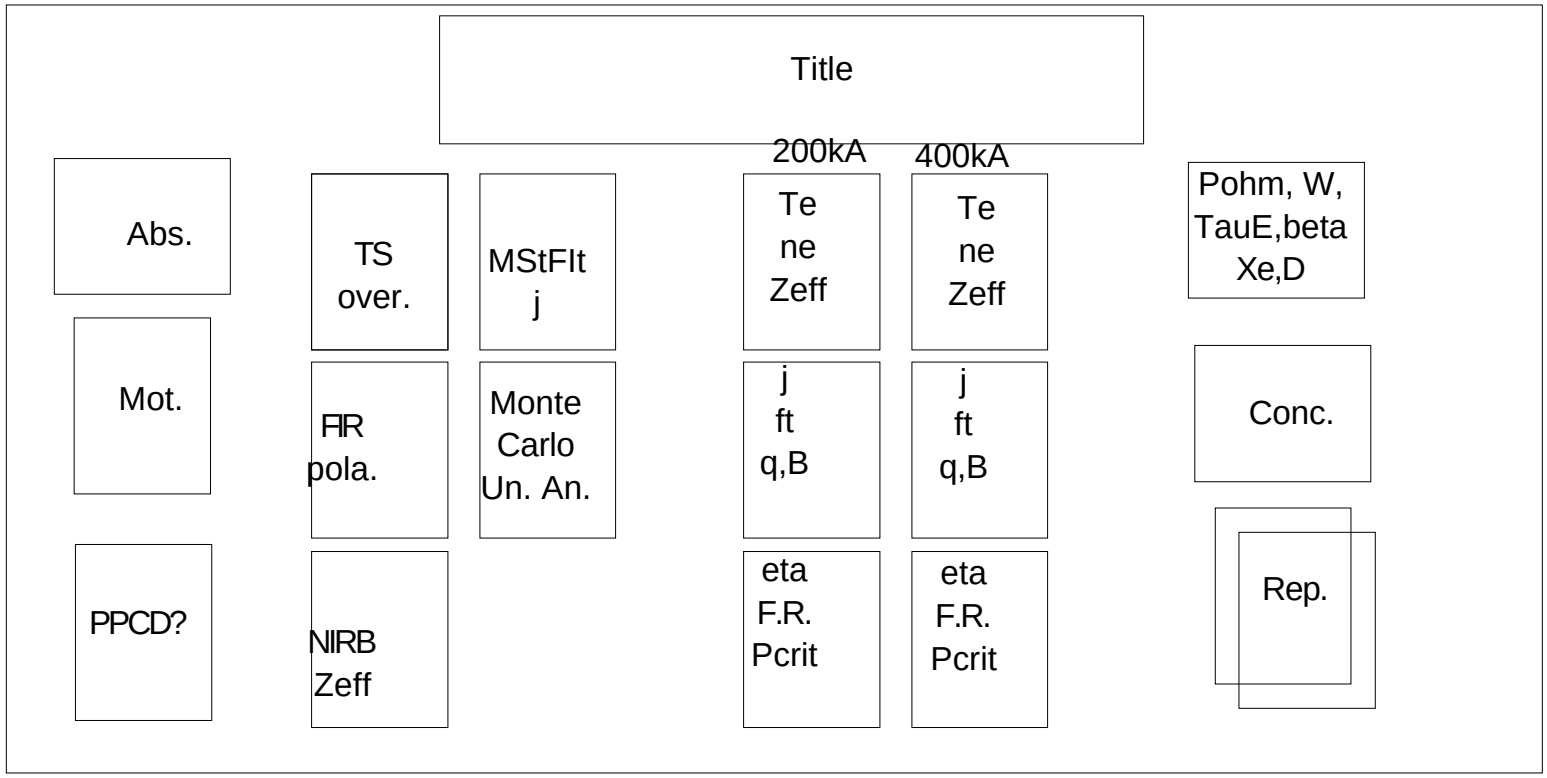

First Quantification of Electron Thermal Transport in the MST Reversed-Field Pinch

T.M. Biewer, J.K. Anderson, B.E. Chapman, N.E. Lanier, S.R. Castillo, D.J. Craig, D.J. Den Hartog, and C.B. Forest
University of Wisconsin-Madison.

Recent diagnostic developments, including an upgrade of the MST Thomson scattering system, have facilitated the first power balance analysis of electron thermal transport in the MST. Recent experiments have focused on acquiring kinetic profile data for electron temperatures and densities under standard and enhanced confinement operating modes. This paper presents results from these experiments, including the first measurement of confinement based upon profile measurements, and a comparison of χ_e for conventional RFP discharges and discharges with inductively modified current profiles. The methodology of the transport analysis begins with 2D equilibrium reconstructions of the current profile and flux surface geometry, constrained by all available magnetic data. Power deposition is calculated from the measured current density profile and estimates of the neoclassical (Hirshman-Sigmar) resistivity (trapped particle corrections to resistivity are found to be significant for 2D RFP equilibria.) Inversions of interferometer data are performed in the flux geometry to determine the electron density profile. Measured electron temperatures from 6 spatial locations are mapped to the flux geometry and fit by spline functions. Ion temperatures (when available from passive spectroscopy of impurity radiation) are similarly constrained. A Monte Carlo uncertainty analysis is done for all results of the transport analysis.

This work was supported by the U.S. D.O.E.

Motivation

- Ongoing improvements to the diagnostic arsenal of the Madison Symmetric Torus have initiated new investigations into the plasma physics of MST transport.

- The use of Pulsed Poloidal Current Drive (PPCD) in the past has demonstrated improved confinement in the MST, based on central electron temperature measurements and a hypothesized profile shape.

- Recent upgrades of the Thomson scattering system have facilitated measurements of the T_e profile in the MST out to r/a=0.88.

- Addition of an NIR Bremstrahlung array has allowed an estimation of Z_{eff} in the MST. **We assume Z_{eff}=2.**

- These measurements, when coupled with density profiles from FIR Interferometry and MSTFIT reconstructed equilibria, have made it possible to calculate many transport quantities, including the electron thermal conductivity χ_e and the energy confinement time τ_E.

- Monte Carlo analysis is used to ascribe error bands for transport quantities, rather than attempting to nonlinearly propagate the experimental uncertainty in the measured data.

What is Pulsed Poloidal Current Drive?

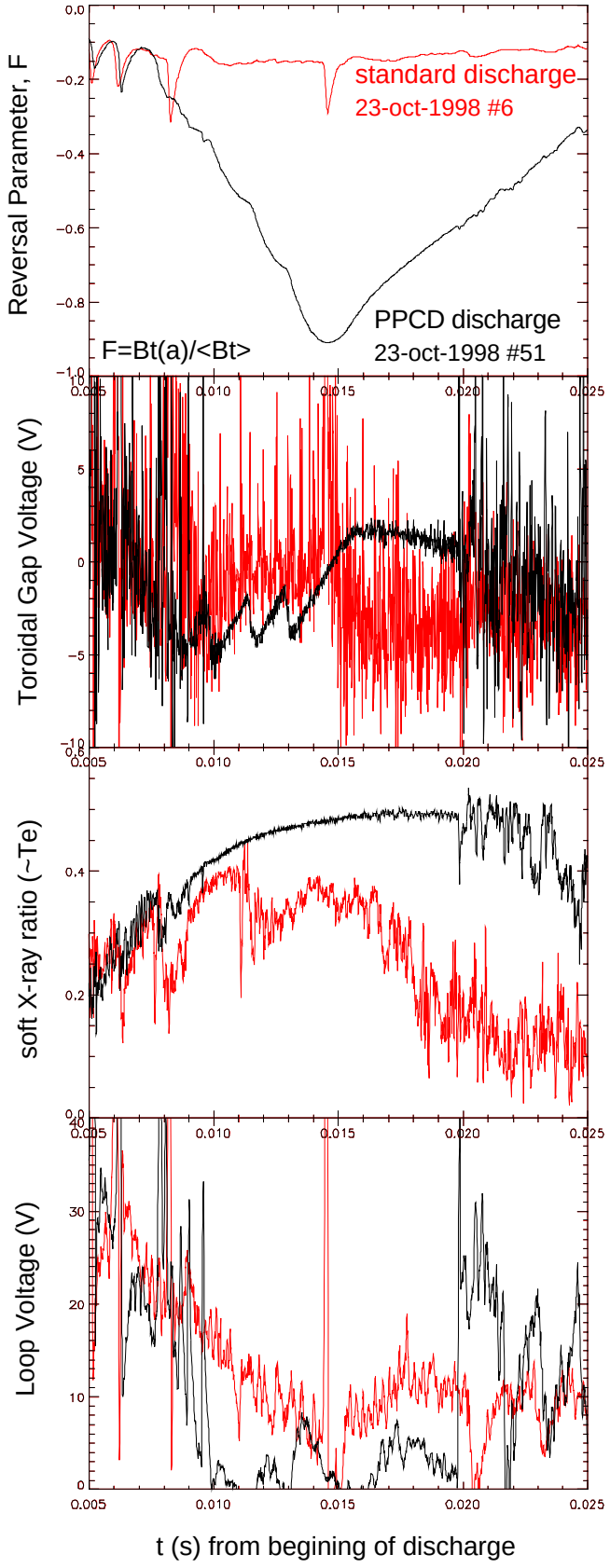

During a "normal" plasma discharge a series of 5 voltage pulses are applied to the MST shell to produce a magnetic field which is in the opposite sense to the established toroidal magnetic field, forcing flux out of the MST. This opposing B is thought to cause a poloidally driven edge current.

PPCD is observed to improve machine performance. It is believed that magnetic modes in the MST derive their free energy from the gradient in the current profile, which is steepest at the edge. By inductively driving current in the edge, PPCD could reduce the gradient and remove free energy from the magnetic modes, resulting in decreased magnetic fluctuations and hence improved particle and energy confinement.

MST Thomson Scattering Diagnostic

5J single-pulse/single-point ruby laser TS system: ensembling of shots (over multiple days) is necessary to construct spacial profiles AND time evolution.

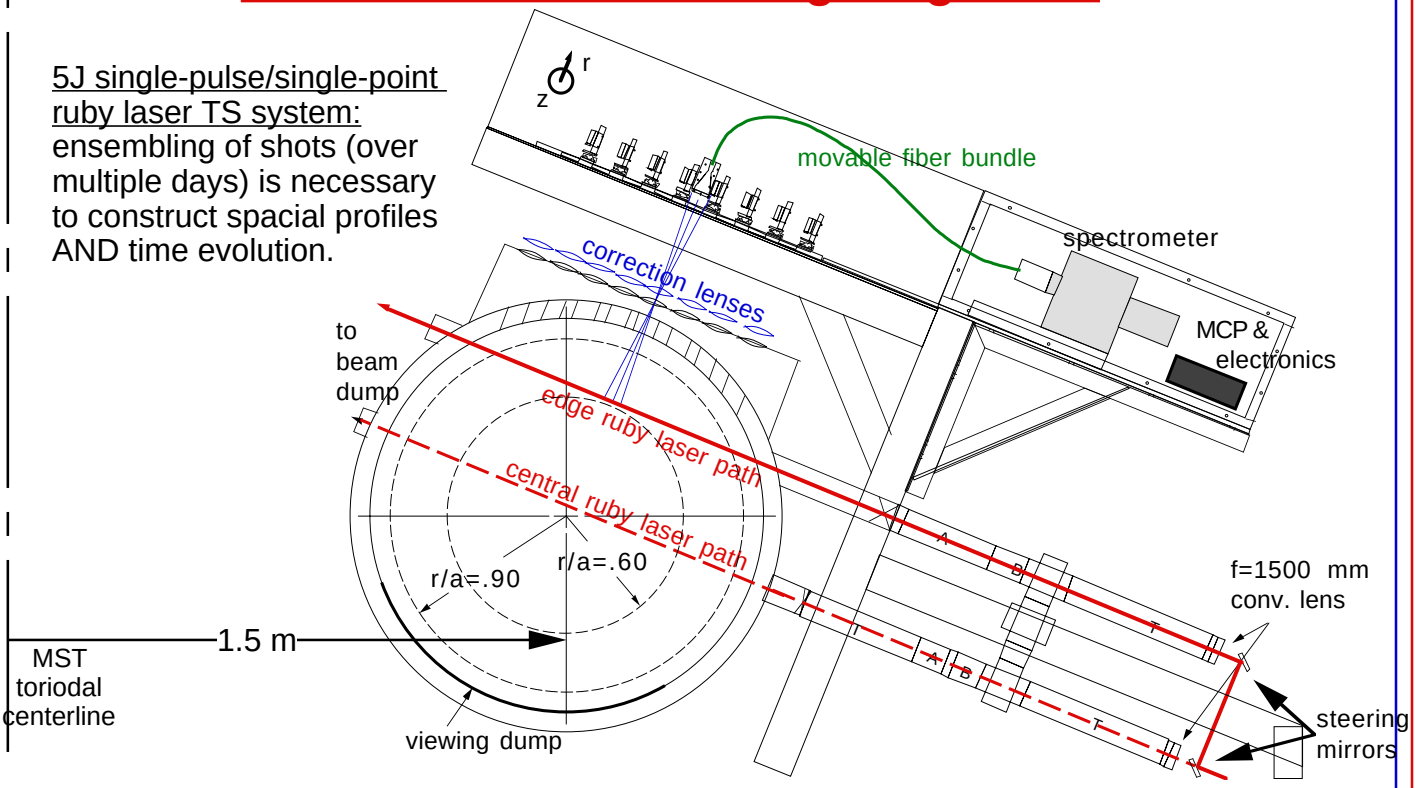

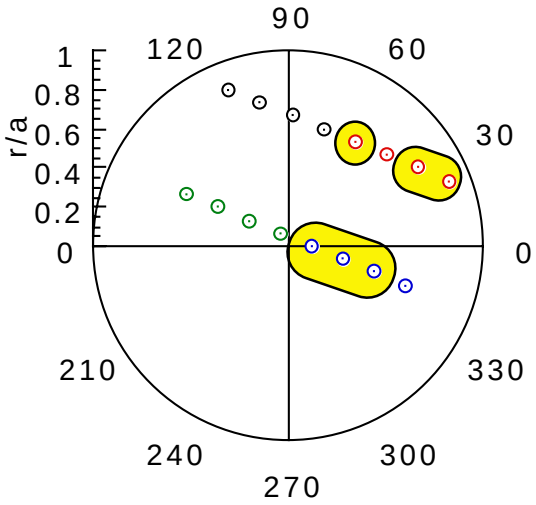

Thomson Scattering Views

view	r/a	ϕ
1	0.627	-18.46
2	0.455	-16.93
3	0.283	-13.53
4	0.115	0
5	0.080	123.91
6	0.244	147.06
7	0.415	151.39
8	0.587	153.19
9	0.882	22.28
10	0.769	31.41
11	0.681	43.26
12	0.630	57.76
13	0.625	73.61
14	0.666	88.59
15	0.746	101.10
16	0.854	110.82

chords used

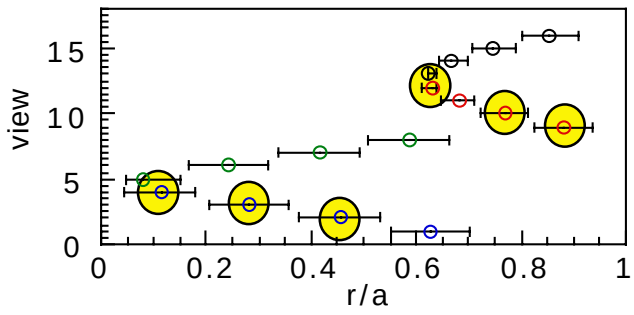

error bars indicate radial range of scattering volume on each view

Far Infrared Interferometer Diagnostic

H_α and Electron Density Profile Measurements on MST

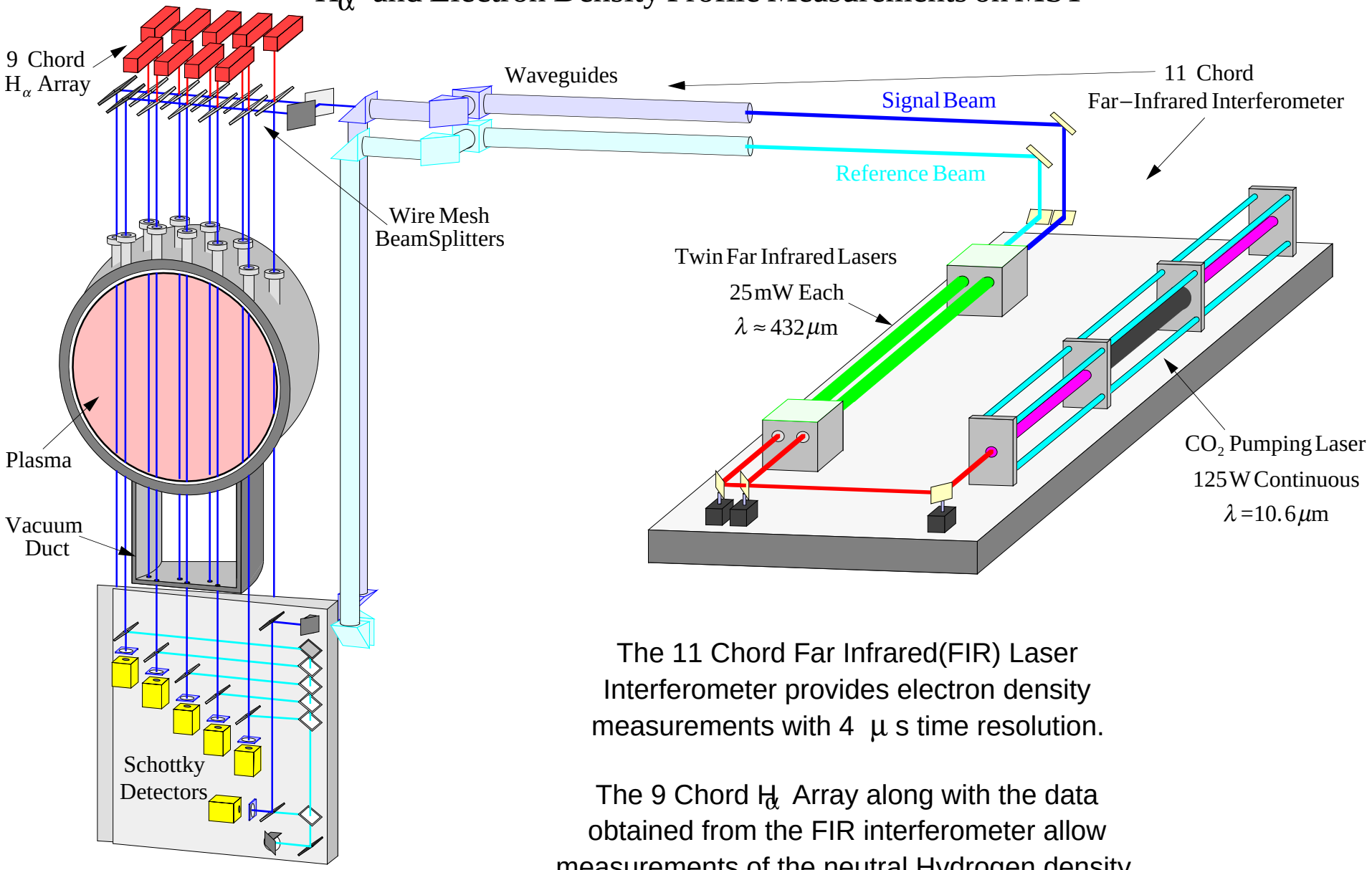

The 11 Chord Far Infrared(FIR) Laser Interferometer provides electron density measurements with 4 μ s time resolution.

The 9 Chord H_α Array along with the data obtained from the FIR interferometer allow measurements of the neutral Hydrogen density.

NIR Bremsstrahlung Z_{eff} Diagnostic

A spectral window in **Bremsstrahlung**'s broadband spectrum - through which other plasma radiative sources (e.g. spectral lines, recombination radiation) are absent or negligible - has been found in the NIR. An array of detectors sensitive to this narrow bandwidth centered at 1040 nm, has been installed on MST.

Poloidal distribution of 17 NIRB Viewing Chords

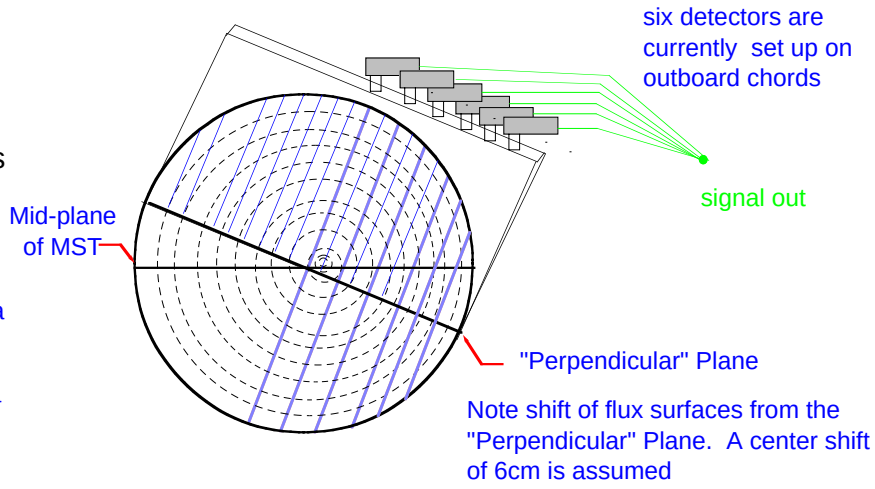

Bremsstrahlung detectors view the plasma through a series of optical lenses.

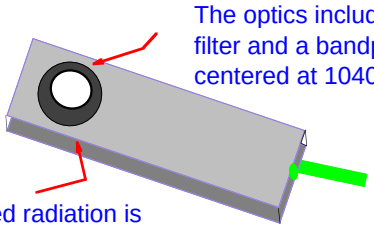

Characteristic NIRB Detector Output

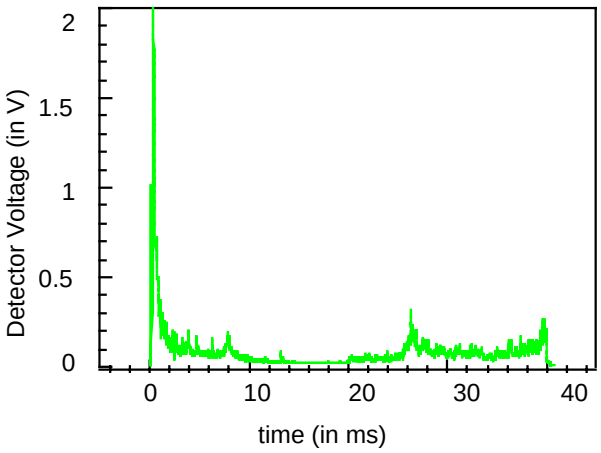

Bremsstrahlung emissivity ( ) can be directly related to Plasma Zeff by the formula:

$$\varepsilon(\lambda) = 1.89 \times 10^{-28} \frac{g_{ff} n^2 Z_{eff} e^{(hc/\lambda T_e)}}{\lambda^2 \sqrt{T_e}}$$

Thus, the detector response (V) across the length (l) of a chord is:

$$V_{det} = \iint F_{cal}(\lambda)\varepsilon(\lambda, l)\, d\lambda\, dl$$

A calibration function (Fcal) has been derived for each detector, but the apparent contamination of recombination radiation at MST's edge (due to lower temperatures) has delayed the data inversions that will produce conclusive Zeff profiles.

Center to Edge Detector Signals

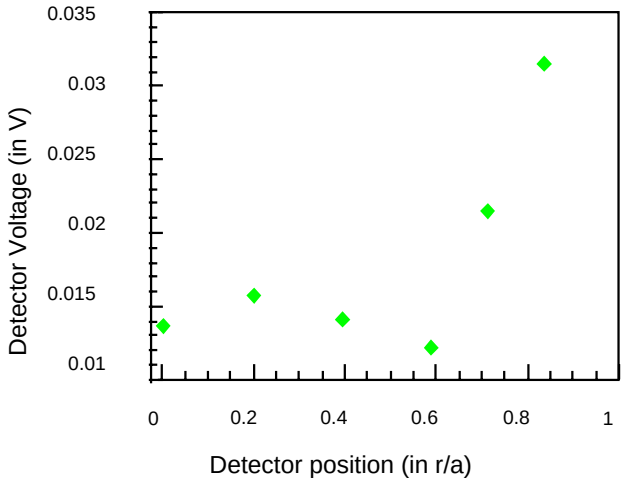

Encouragingly, the raw data displays expected behavior. By selecting appropriate times within each shot, and averaging the signal over an interval, one value (in Volts) is found for each detector in each shot. Here is one such plot of each of the six signals. Note the sharp rise at the edge where recombination radiation dominates and the low emission at the center (as expected for PPCD shots).

MSTFIT is a fully toroidal, 2D equilbrium reconstruction code

Green's function technique is used to relate current and flux

Green's function relates flux to current distribution

$$\psi_{i,j} = \sum_{plasma\ m,n} G_{i,j,m,n} I_{m,n} + \sum_{vessel\ k} G_{i,j,k} I_k$$

$$G(\mathbf{x},\mathbf{x}') = \frac{\mu_0}{\pi k}\left(\left(1-\tfrac{1}{2}k^2\right)K(k) - E(k)\right); k^2 = \frac{4RR'}{(R+R')^2+Z^2}$$

plasma current is modelled by two flux functions

$$I_p(\mathbf{x}) = \frac{F(\hat{\psi}(\mathbf{x}))F'(\hat{\psi}(\mathbf{x}))}{\mu_0 R(\mathbf{x})} + R(\mathbf{x})P'(\hat{\psi}(\mathbf{x}))$$

data are also linearly related to current distribution for example

flux: $$\psi_v = \sum_{plasma\ m,n} G_{v;m,n} I_{m,n} + \sum_{vessel\ k} G_{v;k} I_k$$

probes: $$B_{\theta_p} = \sum_{plasma\ m,n} \left.\frac{\partial G}{\partial n}\right|_{p,m,n} I_{m,n} + \sum_{vessel\ k} \left.\frac{\partial G}{\partial n}\right|_{p,k} I_k$$

Solution is obtained by successive approximations for flux on plasma grid

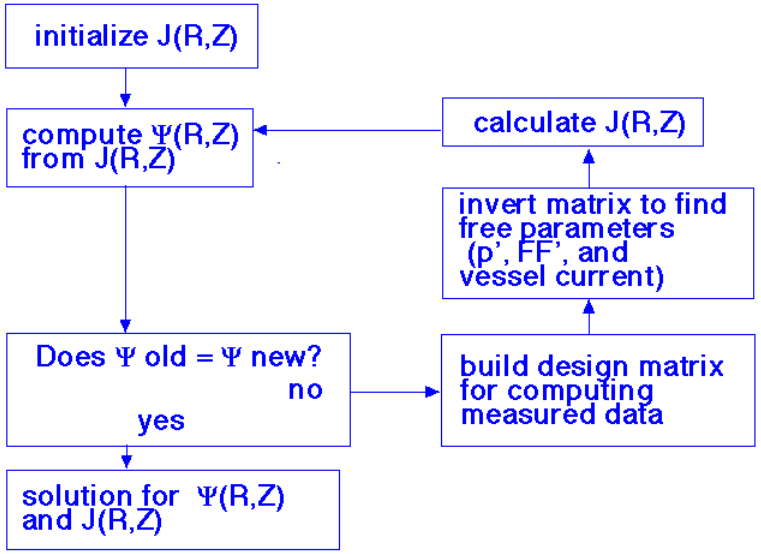

Current profile is specified by Grad-Shafranov equation

$$J_\varphi = \frac{FF'}{\mu_0 R} + Rp'$$

- FF' and p' are the free functions, profiles need to specified to determine toroidal current density
- MSTFit uses free parameters to determine each profile using basis functions.

$$F'(\hat{\psi}) = F_0'(\hat{\psi}) + \sum_n a_n F_n'(\hat{\psi}) \qquad P(\hat{\psi}) = \sum_n b_n P_n(\hat{\psi})$$

MSTFIT also uses free parameters to specify the current distribution in the vessel

Splines are used as the basis functions to construct profiles

- The i-th basis function is given by the spline of a unit height at the i-th knot location with all other knot values set to 0.
- Knot locations are pre-determined to well represent typical RFP profiles.
- The linear combination of the basis functions identically reproduces the spline interpolation of all values.

MSTFIT and Monte Carlo Error Analysis

- MSTFIT is a fully toroidal (2D) equilibrium reconstruction code that utilizes measured data to constrain the reconstruction.

- Plasma Parameters: F, θ, and I_p are entered along with edge magnetic probe signals to manage the reconstruction of equilibrium quantities.

- Once an equilibrium is found, it becomes easier to invert chord averaged quantities, such as FIR measured electron density. The inversions are done in flux coordinate geometry, which can differ significantly from machine geometry.

- Diagnostic data such as T_e, T_i, n_e, dT_e/dt, dn_e/dt, and Z_{eff} are then combined with reconstructed quantities to ultimately calculate profiles of transport coefficients.

- By randomly varying the measured quantities within their error bars and collecting the calculated transport quantities, a Monte Carlo type "error band" is derived.

Measured Profiles

Ip~200 kA

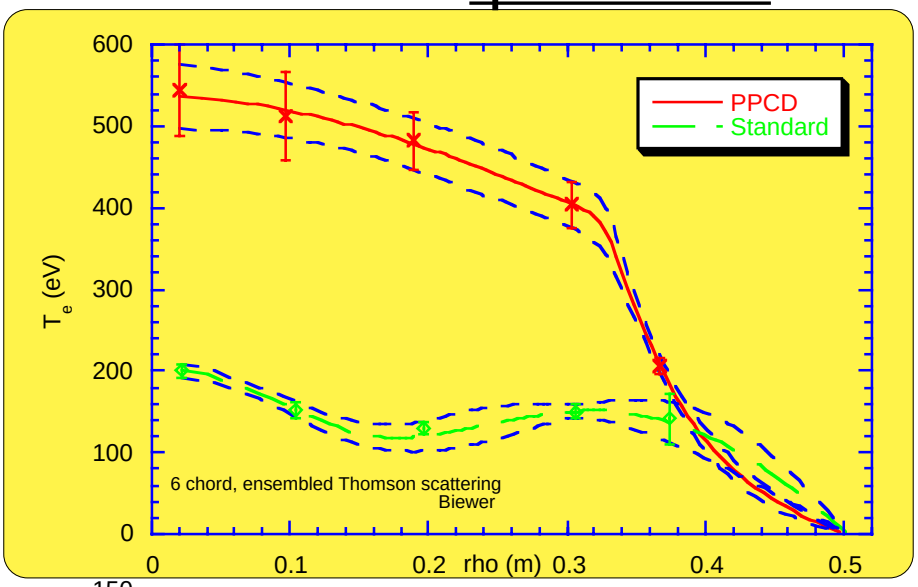

First 6 point electron temperature profiles measured on the MST.

Thomson Scattering measurements are assembled over multiple days and are susceptible to changes in machine conditions.

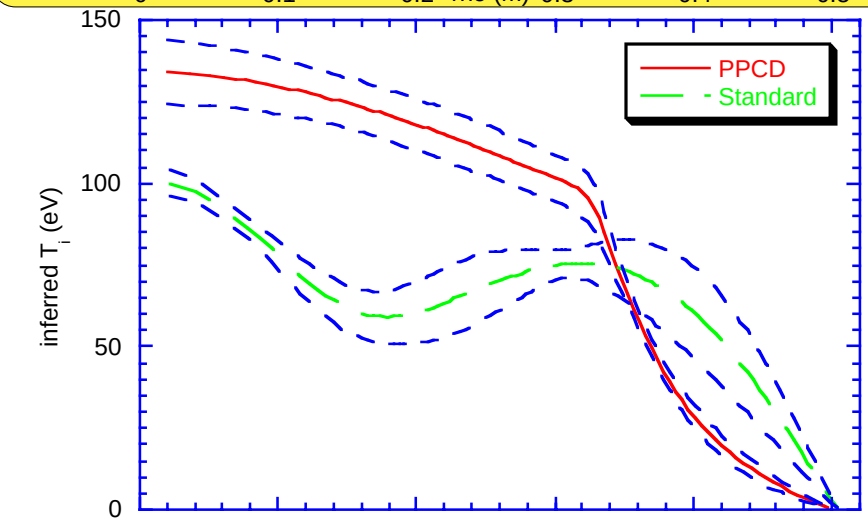

The assumptions that Ti=1/4 Te for PPCD and Ti=1/2 Te for Standard discharges are supported by measurements from majority and minority impurity diagnostics.

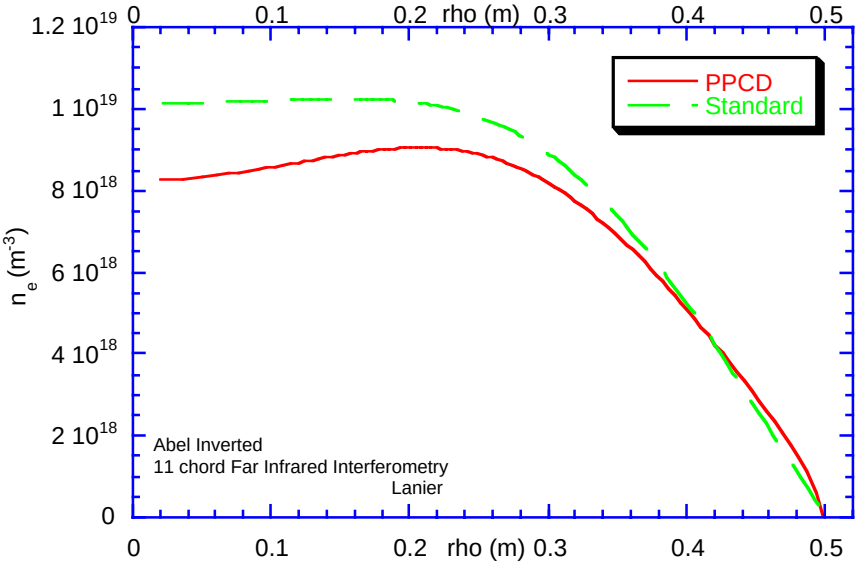

FIR Interferomety measured density profiles are Abel inverted using MSTFIT, a fully toroidal equilibrium reconstruction code.

Measured Profiles

Ip~400 kA

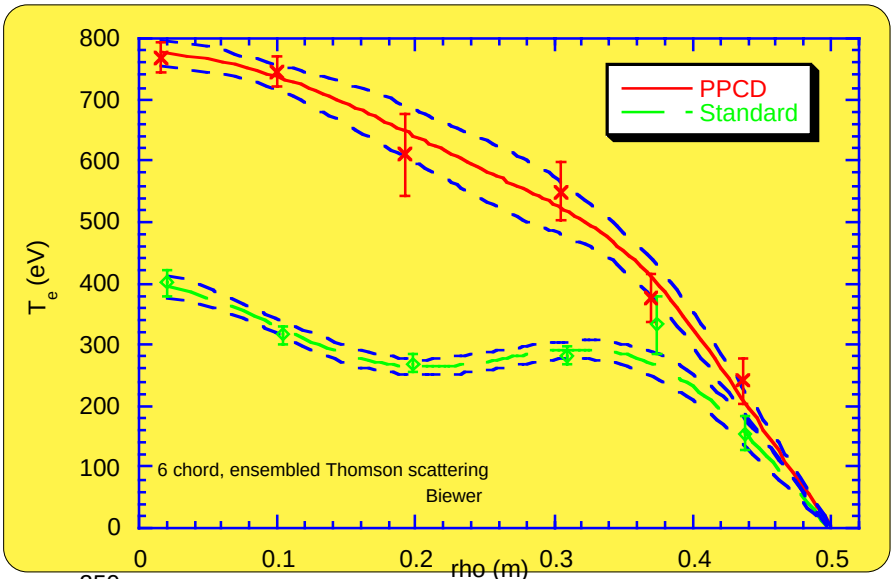

First 6 point electron temperature profiles measured on the MST.

Thomson Scattering measurements are assembled over multiple days and are susceptible to changes in machine conditions.

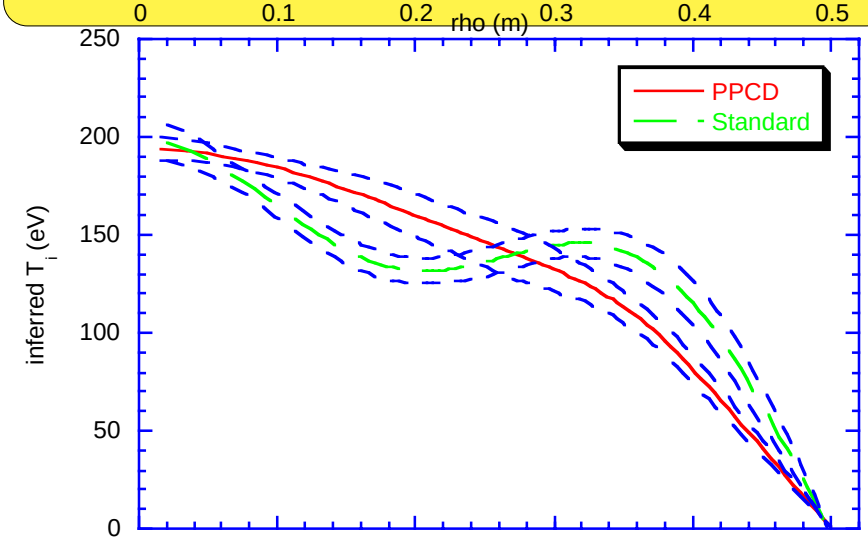

The assumptions that Ti=1/4 Te for PPCD and Ti=1/2 Te for Standard discharges are supported by measurements from majority and minority impurity diagnostics.

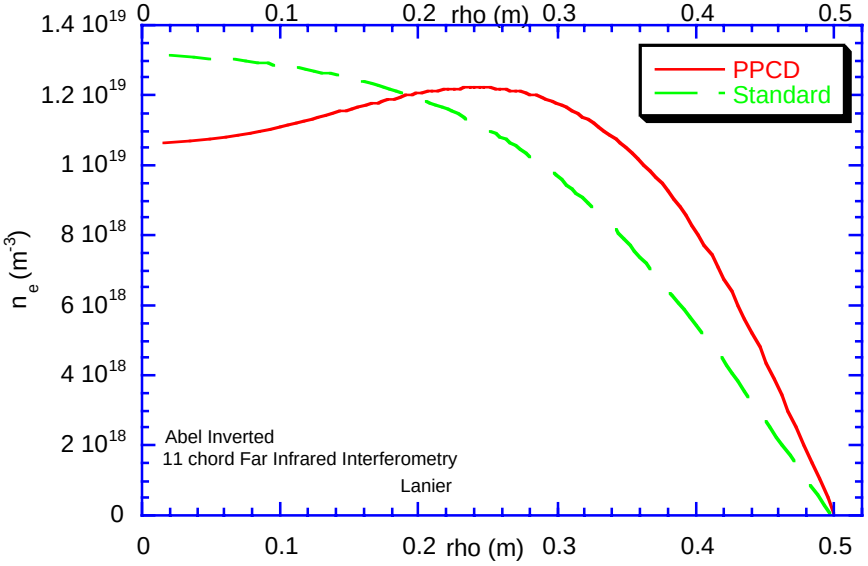

FIR Interferomety measured density profiles are Abel inverted using MSTFIT, a fully toroidal equilibrium reconstruction code.

Reconstructed Profiles

Ip~200 kA

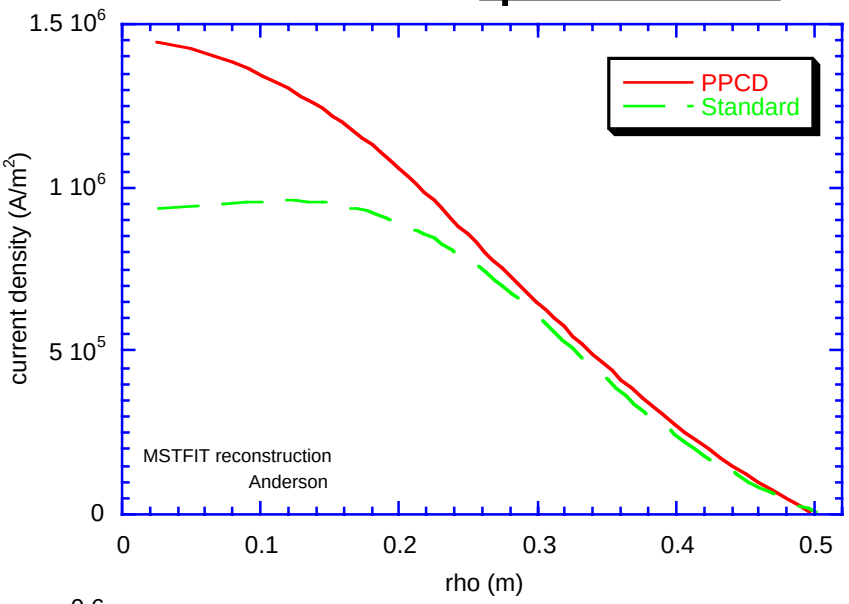

The current density on axis clearly increases, whereas in the edge there is little apparent change.

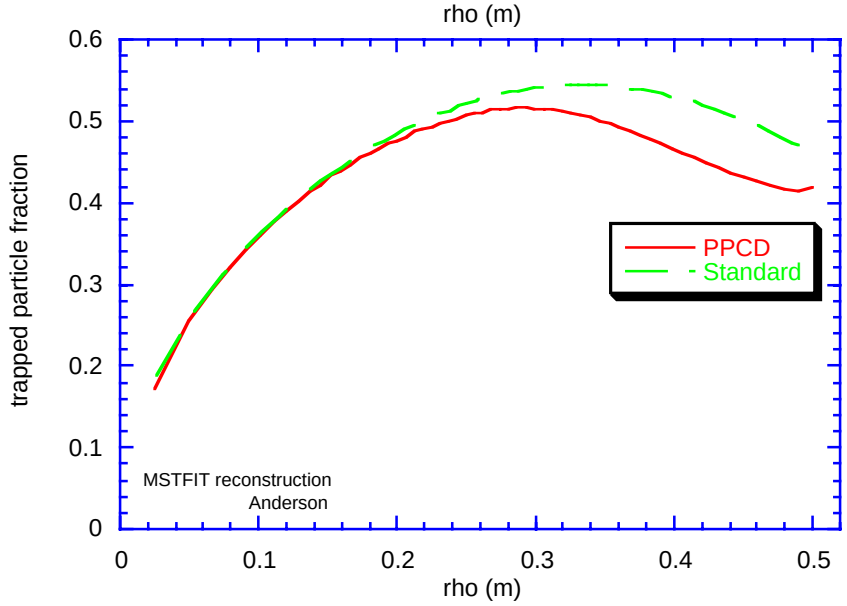

MSTFIT predicts that a substantial fraction of the particles are magnetically trapped in the MST during both PPCD and Standard discharges.

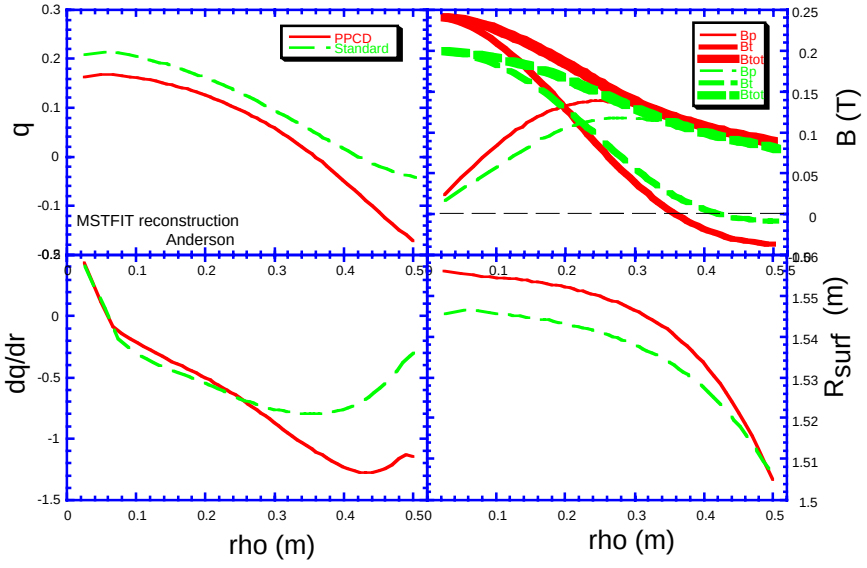

The application of PPCD clearly shifts the flux reversal surface inward, as shown by observing the zero crossing of the toroidal magnetic field.

Also, PPCD leads to an increase in the amount of magnetic sheer at the edge of the plasma.

Reconstructed Profiles

Ip~400 kA

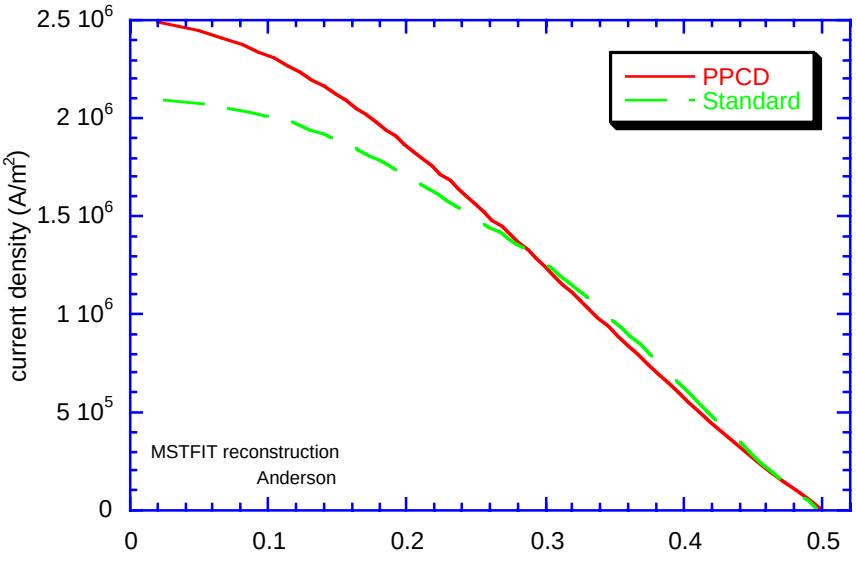

The current density on axis clearly increases, whereas in the edge there is little apparent change.

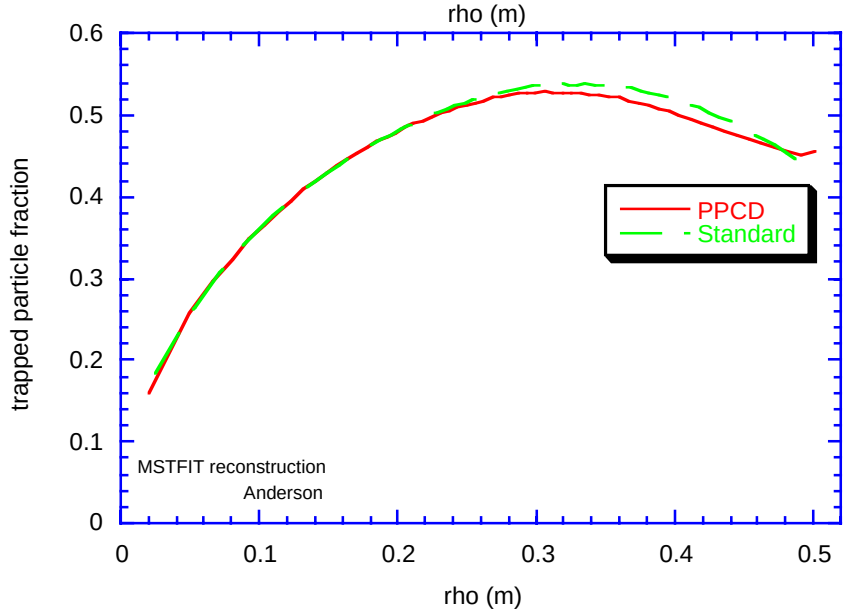

MSTFIT predicts that a substantial fraction of the particles are magnetically trapped in the MST during both PPCD and Standard discharges.

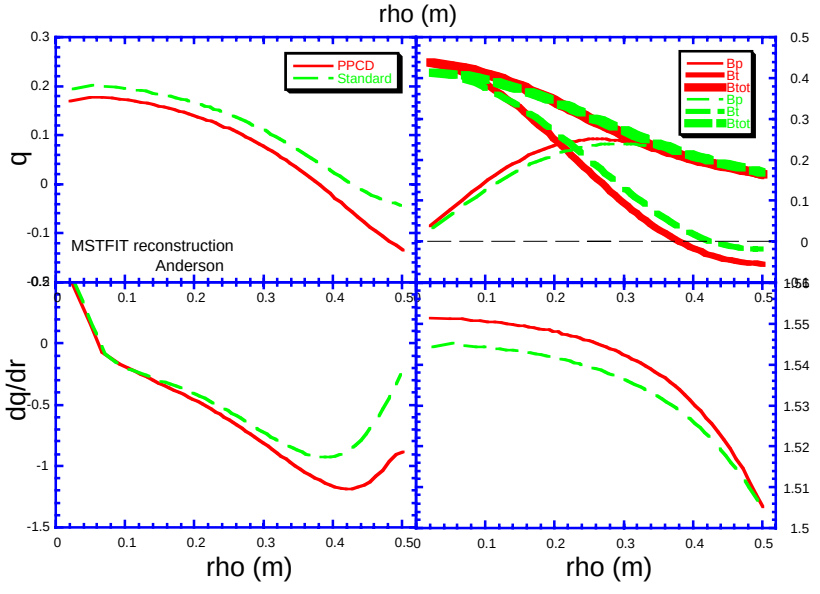

The application of PPCD clearly shifts the flux reversal surface inward, as shown by observing the zero crossing of the toroidal magnetic field.

Also, PPCD leads to an increase in the amount of magnetic sheer at the edge of the plasma.

Calculated Profiles

Ip~200 kA

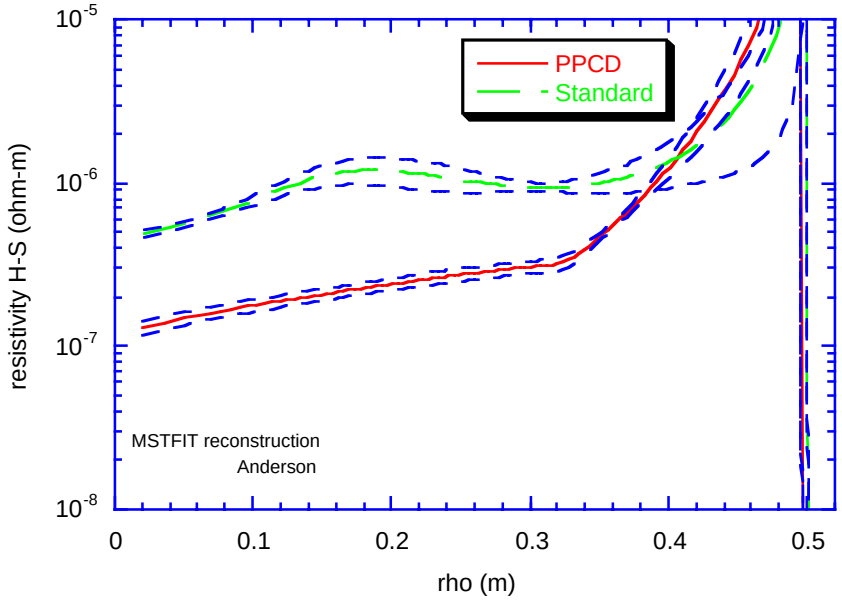

Neoclassical effects become very important when modeling in 2D. Using Hirshman-Sigmar resistivity (rather than Spitzer) in "Standard" reconstructions matches the measured and calculated ohmic input power with a conservative estimate of Zeff=2. I.e. No need of "anomalous" resistivty to account for MHD dynamo action.

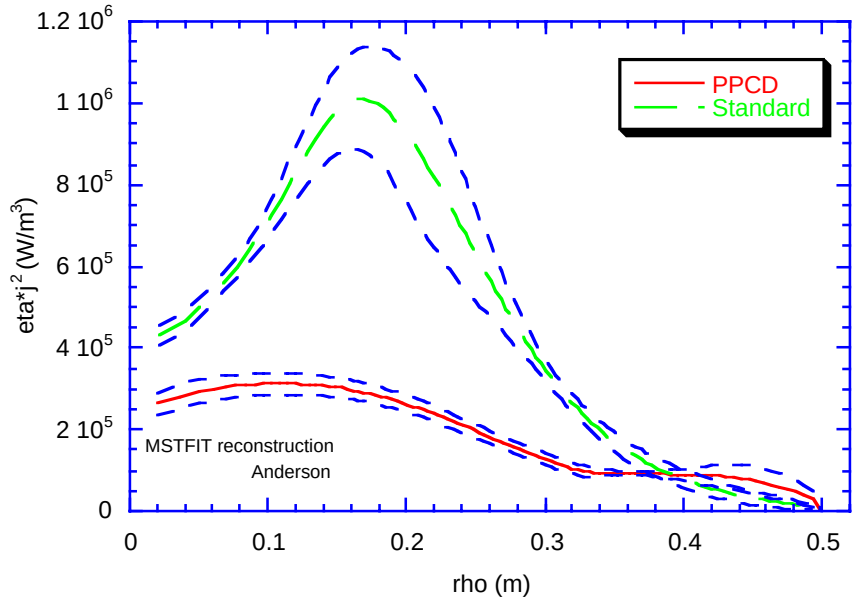

Normalizing to total input power shows that power deposition is **enhanced in the edge during PPCD** as compared to Standard dischages at this current.

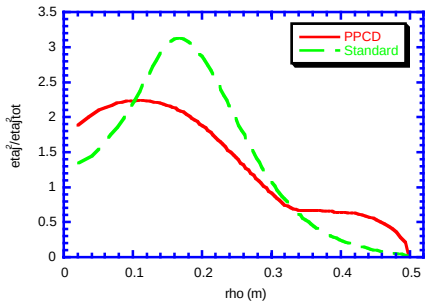

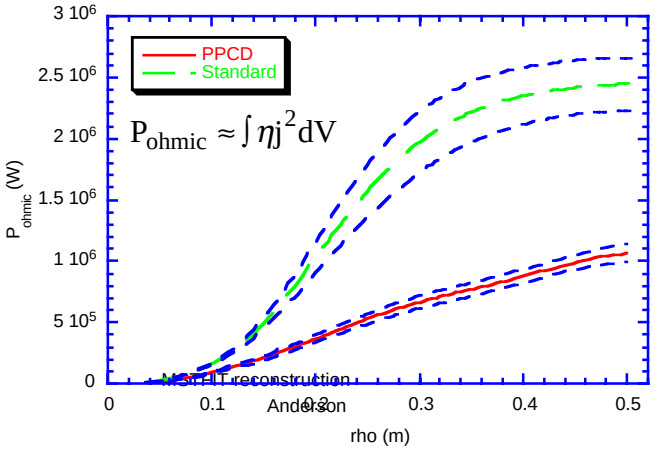

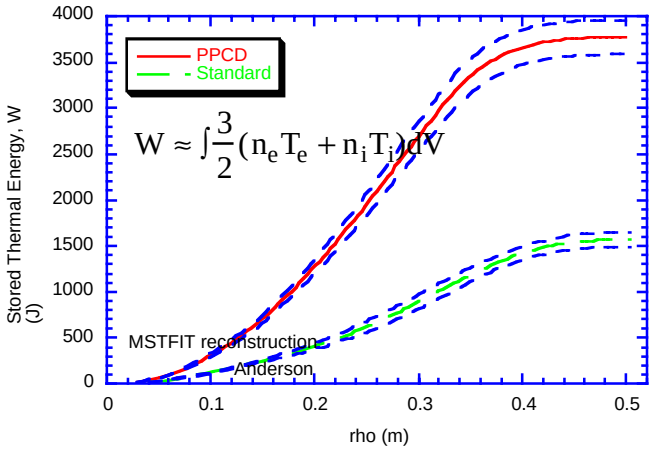

Calculated Profiles

Ip~400 kA

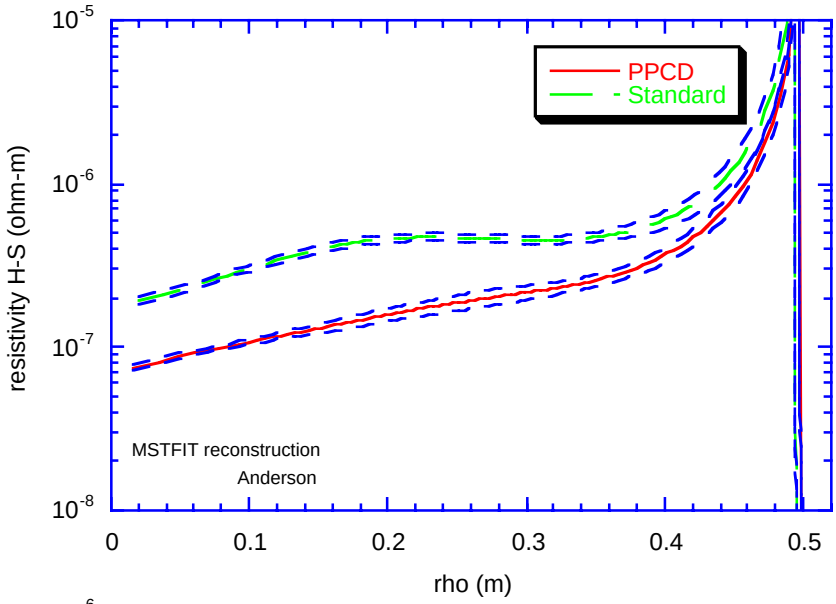

Neoclassical effects become very important when modeling in 2D. Using Hirshman-Sigmar resistivity (rather than Spitzer) in "Standard" reconstructions matches the measured and calculated ohmic input power with a conservative estimate of Zeff=2. I.e. No need of "anomalous" resistivty to account for MHD dynamo action.

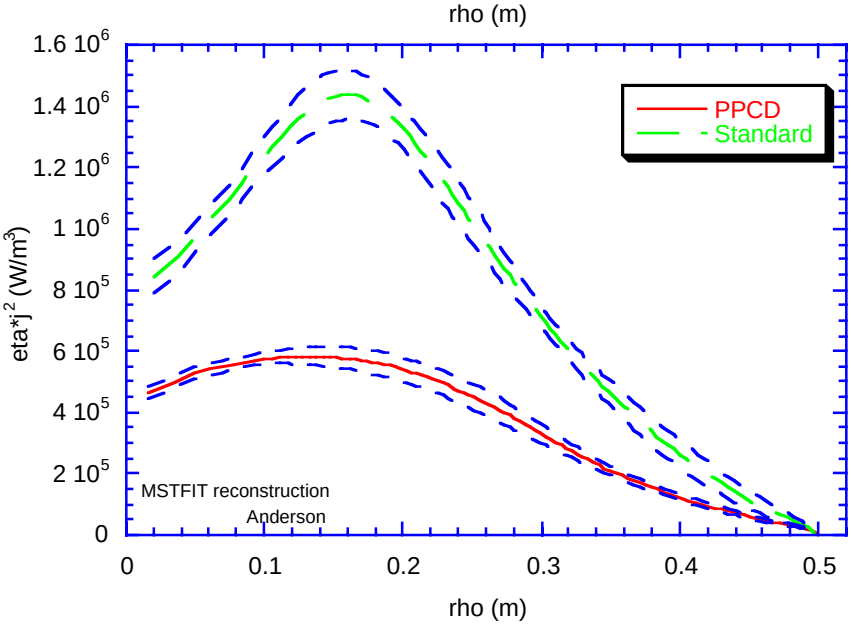

Normalizing to total input power shows that the power deposition profile is nearly identical during PPCD and Standard dischages at this current.

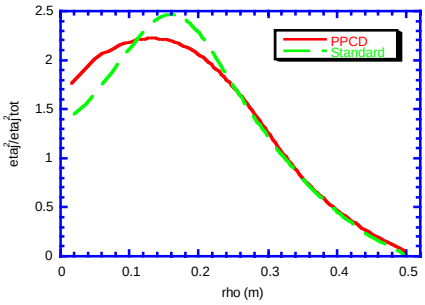

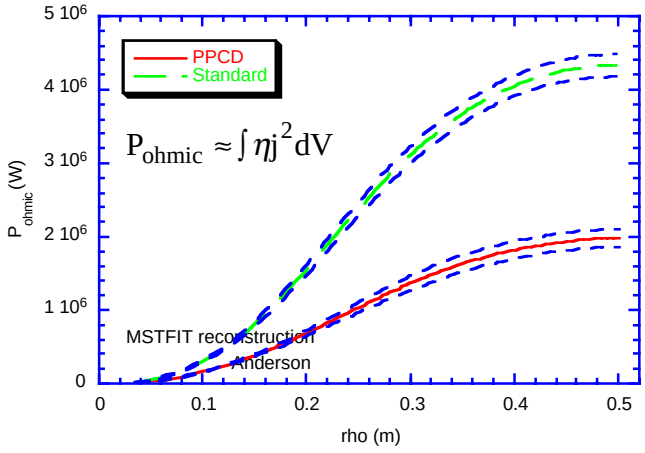

$$P_{ohmic} \approx \int \eta j^2 dV$$

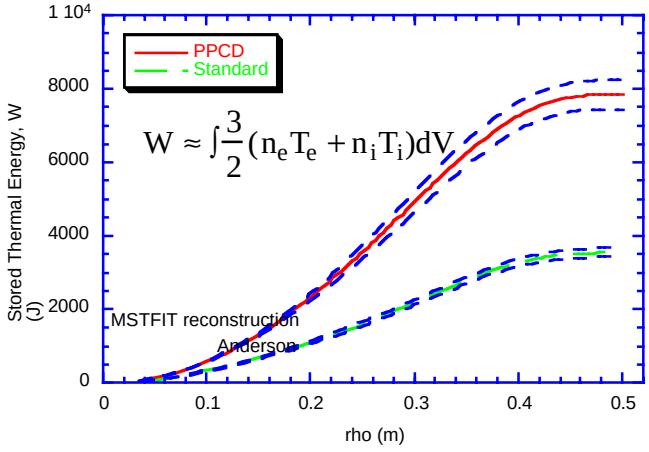

$$W \approx \int \frac{3}{2}(n_e T_e + n_i T_i) dV$$

Main Results

200 kA

	Standard	PPCD	
Pohmic	2.45 +/- 0.22	1.07 +/- 0.08	MW
W	2.0 +/- 0.1	4.2 +/- 0.2	kJ
dW/dt		383.1 +/- 28.6	kW
τ_E	0.81 +/- 0.10	6.45 +/- 1.28	ms
β_{pol}	6.36 +/- 0.33	13.28 +/- 0.66	%

$$\tau_E = \frac{W}{P_{ohmic} - \frac{\partial W}{\partial t}}$$

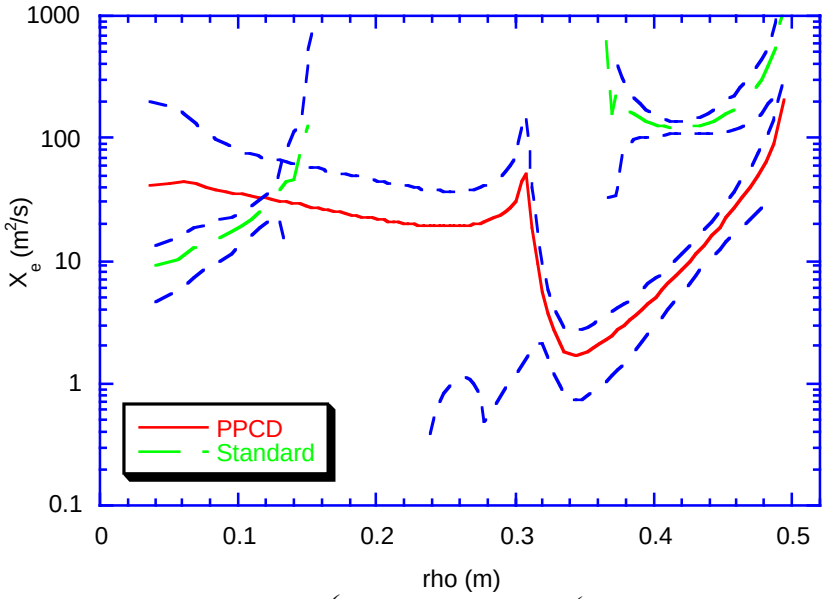

$$X_e \approx \frac{1}{n_e \nabla T_e}\left(\frac{-\int \eta_{HS} j^2 dV + \int \frac{\partial}{\partial t}\left(\frac{3}{2} n_e T_e\right) dV}{4\pi^2 R_0 r} - \frac{5}{2} D_{Class.} T_e \nabla n_e\right)$$

400 kA

	Standard	PPCD	
Pohmic	4.34 +/- 0.16	1.99 +/- 0.12	MW
W	4.4 +/- 0.2	8.8 +/- 0.4	kJ
dW/dt		133.1 +/- 38.1	kW
τ_E	1.02 +/- 0.07	4.83 +/- 0.65	ms
β_{pol}	3.29 +/- 0.11	7.52 +/- 0.38	%

$$\beta_p = \frac{\frac{1}{V}\int (n_e T_e + n_i T_i) dV}{\frac{1}{2\mu_0} B_p^2}$$

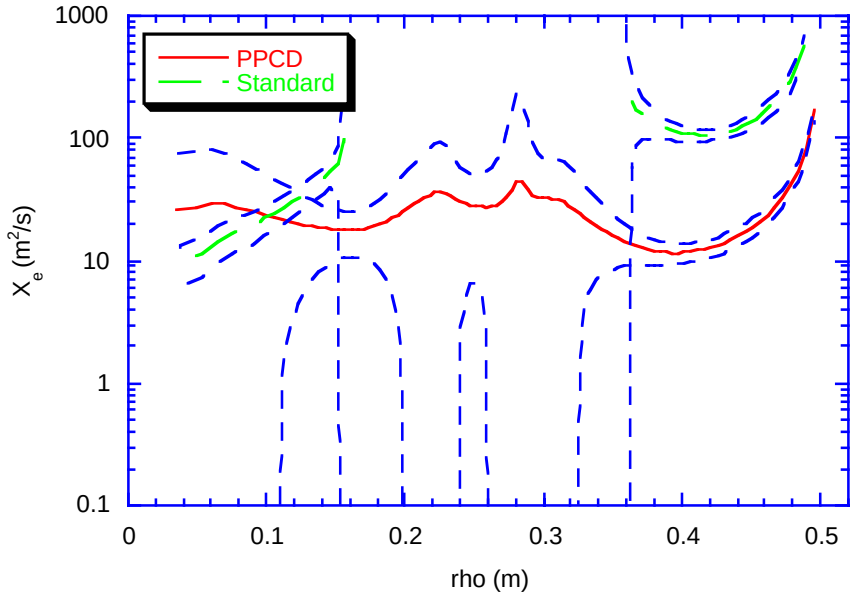

$$D_{Class.} = \frac{\eta_{HS}(n_e T_e + n_i T_i)}{B_{tot}^2} \approx 0.005\ m^2/s$$

for comparison: $D_{Bohm} = \frac{T_e}{16 e B_{tot}} \approx 100\ m^2/s$

Conclusions

- For the first time, 6 point **profiles of T_e have been measured** during PPCD in the MST.

- **Low X_e in the edge is coincident with enhanced magnetic shear in the edge**. During PPCD the flux surface where toroidal magnetic field reverses direction is forced inward (i.e. F is deepened), leading to a steepening of the q profile, particularly in the edge.

- It is **unnecessary to invoke any anomalous resistivty during "standard" MST discharges** if the fraction of trapped particles is taken into account, along with a neoclassical (as per Hirshman and Sigmar) assessment of resistivity**.** With a very reasonable estimation of Zeff=2 the reconstructed input power matches the measured input power.

- **The energy confinement time greatly improves during PPCD**, presumably due to the reduction of magnetic fluctuations.

τ_E**~6 ms** (if Z_{eff}~2) from 1 ms

- β_p **reaches 13% during low current PPCD.**